Compact Bragg Grating Stabilized Ridge Waveguide Laser Module With a Power of 380 mW at 780 nm

Simon Rauch and Joachim Sacher, *Member, IEEE*

***Abstract*— A single ridge waveguide laser wavelength stabilized by a compact external Bragg grating cavity with an output power as much as 380 mW and a beam quality factor M^2 of 1.3 is presented. A characterization concerning tunability by current, short-term optical linewidth, and intensity fluctuations is performed. The device exhibits a wavelength tuning factor at 780 nm of 0.5 pm/mA, a short-term optical linewidth of 18 kHz, and a low-frequency relative intensity noise of –136 dB/Hz. These characteristics allow a high resolution absorption spectroscopy of the D2 line of rubidium.**

***Index Terms*— Semiconductor device packaging, Diode lasers, Laser stability, Bragg gratings.**

EXTERNAL cavity diode lasers (ECDLs) operating in the near infra-red spectral range became a standard tool in the field of atomic physics as well as in bio-medical applications. This is due to a narrow linewidth [1], precise frequency selectability, high power in the order of 100 mW as well as the excellent side mode suppression of 50 dB and higher of ECDLs. They are applied for atom cooling and trapping [2], [3], high precision spectroscopy for establishing laser optical frequency standards [4], quantum information and Raman spectroscopy [5]. However, advanced applications require a narrow linewidth below 100 kHz as well as high output power on the several hundred mW regime [6]. Furthermore, applications of conventional ECDLs in Littrow [7] as well as in Littman/Metcalf [8] configuration suffer from their sensitivity on ambient conditions as there are vibrations, acoustics, and temperature variations. Approaches via Distributed Bragg Reflector (DBR) structures [9] as well as via Volume Holographic Gratings (VHGs) [10], [11] have been chosen for overcoming these issues of conventional ECDLs and Distributed Feedback (DFB) lasers [12].

VHGs consisting of photo-thermo-refractive glass with a high damage threshold, however, have proven to be able to simplify external-cavity configurations [13]. Placing a reflective VHG in front of the laser diode with the grating period perpendicular to the light propagation helps minimize the packaging size. This VHG-based external cavity design is a convenient means used to stabilize high-power arrays of broad area [14] or tapered [15] diode lasers. Such high power ECDLs have been applied for rubidium (Rb) laser pumping at 780 nm [16] and optical pumping of delta oxygen at 763.8 nm [17]. Regardless of the high output power of these diode laser arrays, they can hardly be used for high-precision manipulation of atoms and particles since they suffer from a broad spectral linewidth and a non-Gaussian, low-brightness beam profile with a poor spatial coherence.

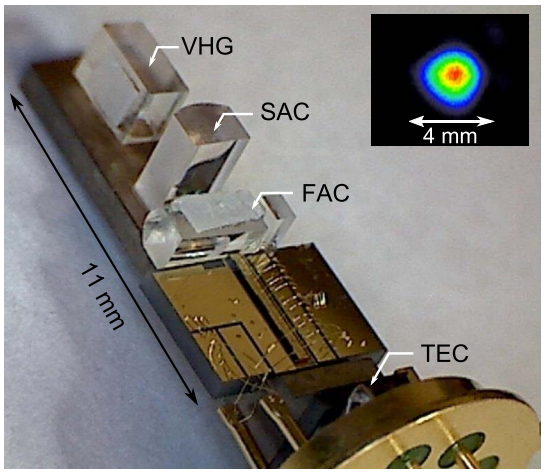

Fig. 1. Compact VHG stabilized ECDL in a TO39 packaging: The whole cavity setup is mounted on a metal plate, which is temperature-stabilized by a thermo-electric cooler (TEC). The divergent beam from the laser diode chip is collimated by a fast and a slow axis collimator lens (FAC), (SAC) to be able to optimize both axis separately. A fraction of the output intensity is reflected back from within the VHG into the laser diode. The total cavity length amounts to 11 mm. The inset depicts the transverse output beam profile, measured at 1.1 m distance to the laser.

In this document we investigate an easy-to-use, compactly packaged VHG stabilized single ridge waveguide laser with a nearly diffraction-limited output beam with an output power as much as 380 mW at an operating wavelength of 780 nm. We investigate the output power along with the wavelength characteristics with respect to a gain current sweep. Moreover, we determine the short-term optical linewidth in a beat measurement of two identical lasers. Finally we demonstrate the spectral purity with a high-precision Doppler-free absorption spectroscopy of Rb vapor.

The ECDL design in a TO39 packaging including a thermo-eletric-cooler (TEC), the laser chip, collimation lenses and a VHG is depicted in Fig. 1. The TO39 can has an overall length of 32 mm and a diameter of 10 mm. The employed laser diode chip is 3.9 mm long and soldered on an AlN heatsink. The device's vertical structure consists of a GaAsP single quantum well active region surrounded by doped 800 nm $Al_{0.4}Ga_{0.6}As$ waveguide layers, which are in turn wrapped by a $Al_{0.85}Ga_{0.15}As$ cladding layer on top and a

Manuscript received January 6, 2015; revised May 1, 2015; accepted May 24, 2015. Date of publication June 1, 2015; date of current version July 10, 2015.

The authors are with Sacher Lasertechnik, Marburg 35037, Germany (e-mail: simon.rauch@sacher-laser.com; jsacher3@gmail.com).

Color versions of one or more of the figures in this letter are available online at http://ieeexplore.ieee.org.

Digital Object Identifier 10.1109/LPT.2015.2438545

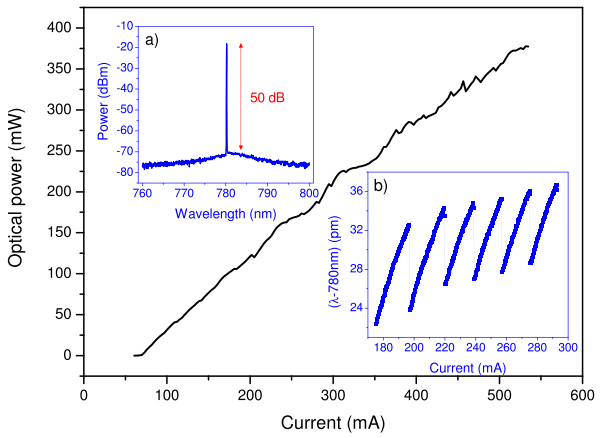

Fig. 2. Light-current characteristics of the ECDL: The total output power is recorded as the injection current is swept upwards. The inset a) depicts the optical spectrum recorded at a current of 400 mA. It shows that the laser operates single mode and the side mode suppression amounts to 50 dB. Inset b) depicts an extract from the sweep, in which the wavelength λ is recorded with a wavemeter. The laser head was stabilized to 15 °C.

$Al_{0.5}Ga_{0.5}As$ layer on the bottom. The output (front) facet of the laser diode is anti-reflection (AR) coated with a reflectivity of 10^{-4} to enable the back reflected light from the VHG enter diode with as low losses as possible, while simultaneously Fabry-Perot modes are suppressed. In contrast, the back facet of the diode is high-reflection coated with a reflectivity above 0.9 to minimize the light leakage.

The laser is run with an in-house developed current source. The laser head temperature is read via a thermistor, located closely to the TEC, and is controlled by an in-house PID controller. Without VHG the threshold current is 113 mA and the gain peak maximum is at a wavelength of 783 nm. For separate collimation of the fast and slow axis we use aspherical cylindrical lenses of a focus length of 1 mm and 2.5 mm, respectively. As a result, an almost diffraction-limited beam profile is obtained. The beam quality factor M^2 has been evaluated by a beam propagation analyzer to $M^2 = 1.3 \pm 0.1$ for both the horizontal and vertical direction.

The VHG is centered around a wavelength of 780.0 nm, has a spectral bandwidth of 0.1 nm and directs a fraction of 12 % of the incoming intensity back to the laser diode. It consists of silicate glass doped with silver, flourine and cerium and has a length of 3 mm. The grating is inscribed holographically via UV light exposure and afterwards thermally cured [18]. According to the Bragg condition, the grating period is 260 nm [19]. The VHG's facets are covered by an AR coating with a residual reflectivity below 0.2 % at 780 nm.

The absolute output power of the ECDL is recorded with the help of an optical power meter after the beam has passed through an optical isolator. The results are shown in Fig. 2. There, one can see that the insertion of the VHG leads to a decrease of the threshold current by 35 mA down to 78 mA. For currents higher than the threshold, the output power rises on average linearly with a slope efficiency of 0.8 W/A. A maximum of 380 mW was obtained at a current of 535 mA. If the gain current is increased further, the TEC current reaches its limit of 1 A so that the system's temperature can no longer be controlled. Consequently a gain current of 535 mA is the limit so far, but an improved heat transfer will help increase the output power in the near future.

The power slope in Fig. 2 exhibits small spikes and is slightly undulated. This behavior can be safely attributed to mode hops: Assuming the laser emits at a pair of longitudinal modes - one from the internal cavity, which is given by the chip itself, and one from the external cavity, which is bounded by the front facet of the diode and the middle of the VHG - the optical length of the laser diode is tuned when the current is swept. Thus the lasing modes of the internal and external cavity drift apart, which causes an undulation of the output power until another pair of modes becomes more resonant and a mode hop occurs [20].

The inset a) in Fig. 2 shows a characteristic optical spectrum for the laser at a current of 400 mA. It is evident that the laser operates in a single mode and the spontaneous emission is suppressed by 50 dB. In the current range above the lasing threshold this side mode suppression ratio (SMSR) remains nearly constant and only features deviations by a maximum of 1 dB. The corresponding evolution of this mode's wavelength is recorded with a wavemeter and is depicted in the inset b) of Fig. 2. There the wavelength changes relative to 780 nm, measured in air, are plotted versus an extract of the laser current sweep. The parallel rising slopes of 0.5 pm/mA illustrate the continuous tuning range. These slopes are interconnected by dotted lines indicating mode hops. The maximum mode-hop-free tuning range amounts to 10.5 pm which is 5.2 GHz.

All measurements of Fig. 2 are obtained at a laser head temperature of 15 °C to demonstrate the system's performance at the rubidium D2 line. If, however, we shift the temperature upwards, the threshold current increases by 1.2 mA/K, whereas the slope efficiency remains constant. Consequently, the output power decreases regarding a fixed gain current value. Additionally, the grating period and thus the lasing wavelength can be tuned by temperature, too. The obtained tuning factor for the wavelength amounts to 10 pm/K. That means a tuning range of 0.2 nm above the rubidium absorption lines around 780.033 nm is accessible by tuning the laser head temperature to 35 °C. An evidence for temperature tuning can also be observed in the inset b) of Fig. 2: The lower edges of the parallel rising slopes are shifted by 6 pm/100 mA, which indicates a temperature difference of 0.6 °C between the TEC and the VHG in that current range. This is because the heat dissipation of the diode chip is asymmetric towards the TEC and the VHG due to different temperature gradients. Hence, a wavelength tuning via the gain current is supported by a tuning via temperature and thus extends the accessible wavelength range.

The power and spectral performance of our system is due to a combination of the long laser chip and a careful selection of the VHG peak reflectivity. A larger VHG reflectivity results in a lower output power and a stronger coupling between the internal and the external resonator and vice versa [21]. Consequently, we chose the VHG reflectivity with regard to output power maximization and a SMSR of at least 50 dB. With comparable VHG stabilized devices similar values of

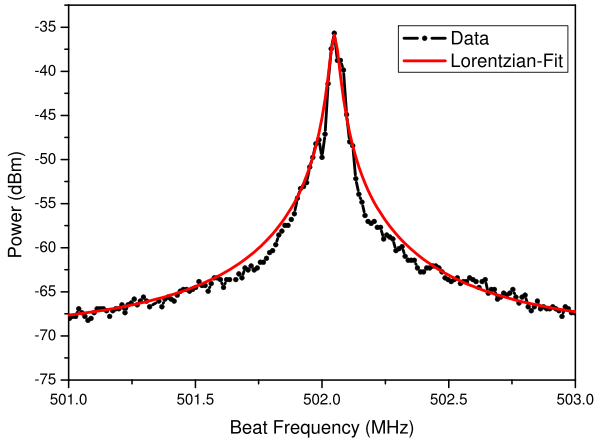

Fig. 3. Experimentally obtained beat note of two identical VHG stabilized ECDLs at 780 nm and the corresponding Lorentzian fit. The 3 dB width amounts to 36 kHz. According to theory [22] the optical linewidth of one the lasers is assumed to be half, i.e. 18 kHz.

45.6 dB [10] and 57 dB [11] were obtained. However, due to the long chip length, our system exceeds the output power at 780 nm of the latter device by a factor of 3.15.

We evaluate the short-term optical linewidth by the beat note of two identically constructed VHG stabilized ECDLs. Their beams are combined via a beam sampler and focused on a photodetector. The amplified photocurrent is evaluated with an electrical spectrum analyzer. The beat note and the corresponding Lorentzian fit are depicted in Fig. 3. The temperature of the laser heads is set to 15 °C and the gain currents are tuned to 216.5 mA and 218.6 mA, respectively, so that their wavelengths differ by 0.5 GHz and the power contribution of 137 mW of each laser is nearly equal. The sweep time is 1 ms/2 MHz. According to [22] the power spectrum of the resulting photocurrent is supposed to fit a Lorentzian shape with a full width at half maximum (FWHM) that equals the sum of the optical linewidths of each laser. Assuming them to be identical, the linewidth of each laser can be derived by dividing the FWHM by two. A Lorentzian fit is performed to the data resulting in a FWHM of 36 kHz with a standard error of ±1 kHz and thus a short-term linewidth of 18 kHz. In order to judge the system's performance, the obtained data is compared to theoretical calculations of the linewidth in [23]. There, the intrinsic linewidth, i.e. the sole laser linewidth excluding current noise, according to [24] is calculated for a comparable DBR laser setup: An intrinsic linewidth down to 2 kHz was found. This value was confirmed experimentally for similar VHG stabilized ECDLs [10], [11]. Therefore, we expect the intrinsic linewidth of our system to be in the same range. The deviation of this intrinsic linewidth from the reported value of 18 kHz is due to residual gain current noise, which is the limiting factor. However, our value is slightly lower compared with the value recently measured with a similar VHG stabilized structure [10]. This is due to the proportional dependence of the linewidth to the inverse mode power [23]–[25].

In order to confirm the performance of the narrow linewidth and the wavelength tuning range a Doppler-free saturation spectroscopy on Rb vapor is performed. The experimental

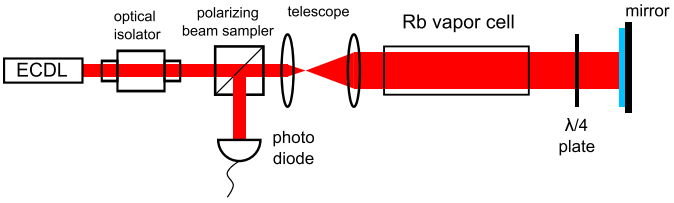

Fig. 4. Double-pass, Doppler-free saturation spectroscopy setup with a Rb vapor cell: The diameter of the horizontally polarized laser beam is first enlarged with a telescope. Then the beam pumps the Rb vapor. Being reflected and passing a $\lambda/4$-plate twice the same beam probes the Rb. Finally the transmitted signal is viewed with a photodetector.

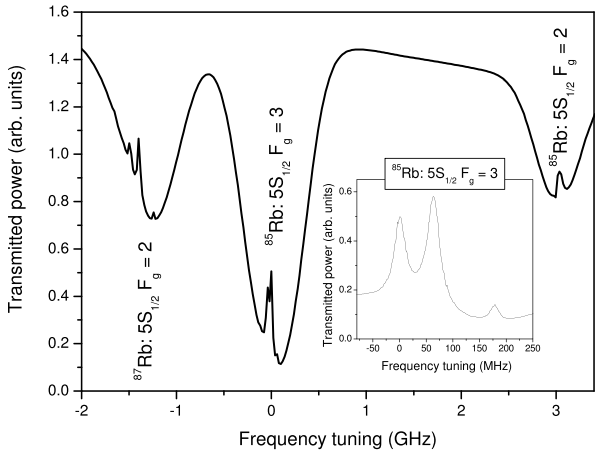

Fig. 5. Saturation absorption spectroscopy with Rb. Within three Doppler-broadened absorption lines the hyperfine structure of Rb can be identified.

setup is shown in Fig. 4. The ECDL is operated at an offset current of 210 mA. Additionally, an AC current with an amplitude of 10 mA and a frequency of 1 kHz is applied. Thus the emission wavelength is continuously tuned by about 5.2 GHz. The diameter of the output beam is first enlarged with a telescope to 1 cm. In this way a large volume of the Rb vapor is pumped. The same beam functions as the probe beam after it has been reflected back and is rotated in polarization by 90°. The transmission signal, now vertically polarized, is led to a photodetector by a polarizing beam sampler and is shown in Fig. 5. Three broad absorption dips can be seen, which belong to the transitions with the following ground states: ^{87}Rb $5S_{\frac{1}{2}}$ $F_g = 2$, ^{85}Rb $5S_{\frac{1}{2}}$ $F_g = 3$ and ^{85}Rb $5S_{\frac{1}{2}}$ $F_g = 2$ [26], [27]. Most importantly, the hyperfine structure Lamb dips can be observed within these three absorption peaks. To confirm this, a high resolution zoom to the dips belonging to the transitions with the ground state ^{85}Rb $5S_{\frac{1}{2}}$ $F_g = 3$ is depicted in the inset of Fig. 5. As a result of the narrow linewidth of our system these dips, which have a typical width in the range of the natural linewidth of Rb (6.07 MHz [27]), are clearly visible.

Since this saturation spectroscopy is usually done in direct detection instead of balanced detection a good signal to noise ratio, i.e. a low intensity noise of the laser, is essential. That is why we evaluate the relative intensity noise (RIN) for a frequency range from 50 Hz to 10 MHz where most microphonic resonances take place. We detect the laser signal with a photodiode and amplify the photocurrent with a

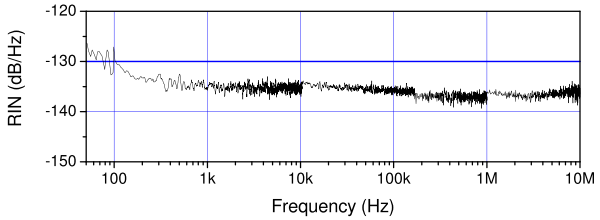

Fig. 6. Relative intensity noise measured with the laser operating at a gain current of 90 mA and a temperature of 15 °C.

transimpedance amplifier. Separated by a bias tee, the AC electrical signal is directed to an electrical spectrum analyzer while the DC power is monitored by a multimeter. The ratio of the AC electrical fluctuations and the DC electrical power, normalized to a resolution bandwidth of 1 Hz, results in the RIN. The obtained results for the laser operating at a current of 90 mA and a temperature of 15 °C are shown in Fig. 6. There, it can be seen that from a frequency of 1 kHz up to 10 MHz the RIN stays at a nearly constant value of –135 dB/Hz to –136 dB/Hz without any resonance spikes due to microphonic effects appearing. This result illustrates an upper limit of the RIN for gain currents higher than the threshold. For tuning the gain current to 150 mA makes the RIN drop by 15 dB. These results once more demonstrate the high mechanical stability of the presented design.

I. Conclusion

We have presented a very compact VHG stabilized external-cavity diode laser. Its output power exceeds the values previously measured for DBR lasers and devices stabilized by VHGs. Furthermore, concerning the narrow linewidth, our laser is an improvement compared with DFB structures and even portrays an alternative to bulky fiber lasers. In addition, our laser concept is very flexible concerning the VHG period and can be easily adapted to different wavelengths in the near infra-red. Along with the presented smooth and reproducible wavelength tunability at high output powers, it thus is an ideal candidate not only for the presented rubidium spectroscopy but also for Raman spectroscopy in mobile and portable operation.

Acknowledgment

The authors would like to thank the Ferdinand-Braun-Institut, Berlin for providing us with laser chips for the experiments.

References

[1] K. Peterman, "External optical feedback phenomena in semiconductor lasers," *IEEE J. Sel. Topics Quantum Electron.*, vol. 1, no. 2, pp. 480–489, Jun. 1995.

[2] R. N. Watts and C. E. Wieman, "Manipulating atomic velocities using diode lasers," *Opt. Lett.*, vol. 11, no. 5, pp. 291–293, 1986.

[3] S. Chu, "Laser manipulation of atoms and particles," *Science*, vol. 253, no. 5022, pp. 861–866, 1991.

[4] C. W. Oates, F. Bondu, R. W. Fox, and L. Hollberg, "A diode-laser optical frequency standard based on laser-cooled Ca atoms: Sub-kilohertz spectroscopy by optical shelving detection," *Eur. Phys. J. D, Atomic, Molecular, Opt. Plasma Phys.*, vol. 7, no. 3, pp. 449–460, Oct. 1999.

[5] K. Sowoidnich, H. Schmidt, M. Maiwald, B. Sumpf, and H.-D. Kronfeldt, "Application of diode-laser Raman spectroscopy for *in situ* investigation of meat spoilage," *Food Bioprocess Technol.*, vol. 3, no. 6, pp. 878–882, Dec. 2010.

[6] A. Rudolf and T. Walther, "Laboratory demonstration of a Brillouin lidar to remotely measure temperature profiles of the ocean," *Opt. Eng.*, vol. 53, no. 5, p. 051407, Jan. 2014.

[7] C. J. Hawthorn, K. P. Weber, and R. E. Scholten, "Littrow configuration tunable external cavity diode laser with fixed direction output beam," *Rev. Sci. Instrum.*, vol. 72, no. 12, pp. 4477–4479, 2001.

[8] M. G. Littman and H. J. Metcalf, "Spectrally narrow pulsed dye laser without beam expander," *Appl. Opt.*, vol. 17, no. 14, pp. 2224–2227, 1978.

[9] B. Sumpf *et al.*, "Wavelength stabilized 785 nm DBR-ridge waveguide lasers with an output power of up to 215 mW," *Semicond. Sci. Technol.*, vol. 29, no. 4, p. 045025, 2014.

[10] E. Luvsandamdin *et al.*, "Micro-integrated extended cavity diode lasers for precision potassium spectroscopy in space," *Opt. Exp.*, vol. 22, no. 7, pp. 7790–7798, Apr. 2014.

[11] E. Luvsandamdin *et al.*, "Development of narrow linewidth, micro-integrated extended cavity diode lasers for quantum optics experiments in space," *Appl. Phys. B*, vol. 111, no. 2, pp. 255–260, May 2013.

[12] D. J. Dougherty, R. C. Gutierrez, S. Dubovitsky, and S. Forouhar, "Semiconductor laser linewidth measurements for space interferometry applications," *Proc. SPIE*, vol. 3626, pp. 115–122, Apr. 1999.

[13] G. B. Venus, A. Sevian, V. I. Smirnov, and L. B. Glebov, "High-brightness narrow-line laser diode source with volume Bragg-grating feedback," *Proc. SPIE*, vol. 5711, pp. 166–176, Mar. 2005.

[14] G. J. Steckman, W. Liu, R. Platz, D. Schroeder, C. Moser, and F. Havermeyer, "Volume holographic grating wavelength stabilized laser diodes," *IEEE J. Sel. Topics Quantum Electron.*, vol. 13, no. 3, pp. 672–678, May/Jun. 2007.

[15] D. Vijayakumar *et al.*, "Narrow line width operation of a 980 nm gain guided tapered diode laser bar," *Opt. Exp.*, vol. 19, no. 2, pp. 1131–1137, Jan. 2011.

[16] A. Gourevitch, G. Venus, V. Smirnov, D. A. Hostutler, and L. Glebov, "Continuous wave, 30 W laser-diode bar with 10 GHz linewidth for Rb laser pumping," *Opt. Lett.*, vol. 33, no. 7, pp. 702–704, Apr. 2008.

[17] L. S. Meng, B. Nizamov, P. Madasamy, J. K. Brasseur, T. Henshaw, and D. K. Neumann, "High power 7-GHz bandwidth external-cavity diode laser array and its use in optically pumping singlet delta oxygen," *Opt. Exp.*, vol. 14, no. 22, pp. 10469–10474, Oct. 2006.

[18] L. B. Glebov, "Volume Bragg gratings in PTR glass–new optical elements for laser design," in *Advanced Solid-State Photonics*. Washington, DC, USA: OSA, 2008, p. MD1.

[19] I. V. Ciapurin, L. B. Glebov, and V. I. Smirnov, "Modeling of phase volume diffractive gratings, part 1: Transmitting sinusoidal uniform gratings," *Opt. Eng.*, vol. 45, no. 1, pp. 015802-1–015802-9, Jan. 2006.

[20] R. Lang and K. Kobayashi, "External optical feedback effects on semiconductor injection laser properties," *IEEE J. Quantum Electron.*, vol. 16, no. 3, pp. 347–355, Mar. 1980.

[21] L. Hildebrandt, R. Knispel, S. Stry, J. Sacher, and F. Schael, "Antireflection-coated blue GaN laser diodes in an external cavity and Doppler-free indium absorption spectroscopy," *Appl. Opt.*, vol. 42, no. 12, pp. 2110–2118, Apr. 2003.

[22] W. Zhou, K. M. Chong, and H. Guo, "Linewidth measurement of Littrow structure semiconductor laser with improved methods," *Phys. Lett. A*, vol. 372, no. 23, pp. 4327–4332, Jun. 2008.

[23] S. Spießberger, M. Schiemangk, A. Wicht, H. Wenzel, G. Erbert, and G. Tränkle, "DBR laser diodes emitting near 1064 nm with a narrow intrinsic linewidth of 2 kHz," *Appl. Phys. B*, vol. 104, no. 4, pp. 813–818, Sep. 2011.

[24] C. H. Henry, "Theory of the linewidth of semiconductor lasers," *IEEE J. Quantum Electron.*, vol. 18, no. 2, pp. 259–264, Feb. 1982.

[25] W. Elsäßer, E. Gobel, and J. Kuhl, "Coherence properties of gain- and index-guided semiconductor lasers," *IEEE J. Quantum Electron.*, vol. 19, no. 6, pp. 981–985, Jun. 1983.

[26] D. A. Steck. (May 2, 2008). *Rubidium 87 D Line Data, Revision 2.0.1*. [Online]. Available: http://steck.us/alkalidata

[27] D. A. Steck. (Sep. 20, 2013). *Rubidium 85 D Line Data, Revision 2.1.6*. [Online]. Available: http://steck.us/alkalidata